Hot-Electron Emission From Shallow p-n Junctions in Silicon*†

D. J. BARTELINK,‡ J. L. MOLL, AND N. I. MEYER§
Stanford Electronics Laboratories, Stanford University, Stanford, California
(Received 17 December 1962)

The energy distribution of hot electrons in silicon has been investigated experimentally and theoretically by observation of the energy distribution of electrons emitted into vacuum from a reverse biased p-n junction 1000 Å below the surface. This emission has been related by means of the Boltzmann transport equation to the mean free paths for optical phonon emission and impact ionization. Two experiments were performed. In the first, with the junction biased to avalanche breakdown, the product of the mean free paths effectively determines the attenuation length for electrons in the resulting nearly Maxwellian distribution. The dependence of the emitted current on the n-layer thickness, which determines the attenuation length, and the field configuration within the junction were determined by removing thin calibrated layers (33 Å) of silicon by boiling water oxidation. The second experiment, in which avalanche breakdown and its complications were avoided by optical generation of carriers, has been analyzed in terms of a plane source of electrons released a known distance below the surface at a given energy. The number of emitted electrons then has a maximum at an energy loss depending on the ratio of the mean free paths. The solution of the transport equation similar to that of Wolff, extended to include the initial transient in a field region, was fitted to the experimental data. A good fit was obtained using mean free paths for optical phonon emission of 60 Å and for impact ionization of 190 Å.

I. INTRODUCTION

THE characteristics of the emission of hot electrons from a semiconductor into vacuum are governed both by the mechanism by which the electrons lose energy, a property of the solid, and by the method of heating the electrons to an energy sufficient for escape. The heating is generally achieved by a strong electric field, such as in a reverse biased p-n junction, and is, therefore, a function of the experimental structure.

Described here are two experiments performed on a silicon structure in which a reverse biased p-n junction was located parallel and close to the surface. The observed attenuation length of 4- to 5-eV electrons was measured nearly independent of the method of generation of the hot electrons. The second experiment consisted of measuring the emitted electron energy distribution which is related to the energy gain and loss mechanisms of electrons traversing a region in which the geometrical parameters are known.

The distance hot electrons will travel before losing too much energy to overcome the potential barrier at the surface is determined by the mean free paths for scattering by the two principal mechanisms: optical phonon emissions and secondary ionizations by collisions with valence band electrons. Electron multiplication in the avalanche breakdown of p-n junctions has been analyzed in terms of these mechanisms but the mean free paths so determined vary widely, depending on how the relative effects of the mechanisms are averaged over the electron energy distribution. Because of this uncertainty and the close relationship between the avalanche breakdown theories and the theory needed to describe the present emission experiments, we will survey briefly the two theories, by Wolff[1] and by Shockley,[2] before describing the emission experiments.

Avalanche Breakdown Theories

The calculation concerns the dependence of the ionization coefficient α_i, the number of secondary electrons produced per unit length, on the field E in a junction. Wolff assumes that the electrons are distributed nearly isotropically in velocity space by expanding the distribution function in the transport equation in terms of spherical harmonics and retaining only the first two terms. The energy distribution he obtains is Maxwellian below the threshold for secondary ionization, $\mathcal{E}_i$. The further assumption that the mean free path for ionization interaction (l_i) is much shorter than that for phonon emission (l_r) and the assumed small anisotropy of the distribution leads to a dependence α_i on E of the same form as the number of electrons above $\mathcal{E}_i$ (which is given by the electron temperature of the Maxwellian distribution below $\mathcal{E}_i$). Wolff finds that $\ln(\alpha_i)$ varies as approximately E^{-2}. The experimental $\ln(\alpha_i)$ for silicon, however, varies very nearly as E^{-1}, indicating that the distribution is perhaps not spherical for silicon in the range of fields obtained in junctions.

Shockley, observing this discrepancy in the E dependence of $\ln(\alpha_i)$, proposed a kinetic theory in which he treats only the deviation from the average of the distribution that describes electrons moving in the field direction. The peak of the energy distribution is assumed to occur at an energy small compared with $\mathcal{E}_i$. Then, an ionization can occur only when an electron can travel a distance $\mathcal{E}_i/qE$ (q is the electronic charge) without any randomizing phonon collisions and can ionize in the first collision once it reaches $\mathcal{E}_i$. The ionization coefficient can

* This work supported in part by Signal Corps Contract DA36(039) SC85339 and in part by Air Force Contract WADD AF33(616)7726.
† Based on a thesis submitted by D. J. B. to Stanford University in partial fulfillment of the requirements of the Ph.D. degree.
‡ Present address: Bell Telephone Laboratories, Murray Hill, New Jersey.
§ Present address: Technical University of Denmark, Copenhagen, Denmark.

[1] P. A. Wolff, Phys. Rev. **95**, 1415 (1954).
[2] W. Shockley, Solid-State Electron. **2**, 35 (1961).

then be calculated in the low-field limitwhen the average energy of the electrons is low and all electrons capable of causing ionization are contained in a sharp spike in the field direction. As was pointed out by Shockley and elsewhere,[3] this low-field limit is exceeded for silicon, indicating that the distribution is not completely peaked in the forward direction, but is partly spherical.

Both theories can be appropriate for materials other than silicon in which the specific limiting forms of the distribution actually exists.[4] The choice of the value of $\mathcal{E}_i$ influences rather strongly the parameters needed by either theory to fit the ionization coefficient data. Together with the uncertainty about the exact shape of the distribution, the somewhat arbitrary choice of $\mathcal{E}_i$ which must be made leaves the mean free paths in considerable doubt. Table I shows the parameters used by Wolff and Shockley, and those required by the present work on electron emission for an explanation of the observed data.

One additional parameter assumed known from independent measurement[5] is the energy loss to optical phonons. The assumption made by Shockley and used here also is that only the zero-wave-vector (Raman) optical phonon, $\mathcal{E}_r=0.063$ eV, can contribute. At low electron energies, however, some intervalley scattering by acoustic phonons may lead to a comparable mean free path. Since these phonons would have wave vectors nearly the value at the zone edge, they would be comparable in energy to $\mathcal{E}_r$. Their effect will be included in the optical phonon effects, although it is unnecessary to consider details of this type when the conduction band structure has been completely neglected in both of the above theories as well as the present work.

Distribution of Emitted Electrons

We now return to a consideration of the effect of collisions on the shape of the distribution of those electrons which are of interest to electron emission and then show how the appropriate conditions are met by the emission structure used. Only electrons with kinetic energies at the surface exceeding the electron affinity ($\psi\cong 3.8$ eV for silicon), and, hence, $\mathcal{E}_i$ can be emitted.

TABLE I. Comparison of fitting parameters required by theories on avalanche breakdown with those of the present work on electron emission.

	Avalanche breakdown		Electron emission
	Wolff	Shockley	Present work
l_r (phonons)	200 Å	50 Å	60 Å
l_i (ionization)	20 Å	880 Å	190 Å
$\mathcal{E}_i$ (threshold)	2.3 eV	1.1 eV	···
$r=l_i/l_r$	0.1	17.5	3.2

[3] J. L. Moll and N. I. Meyer, Solid-State Electron. **3**, 155 (1961).
[4] Since the completion of the present work a more complete theory of avalanche breakdown covering the range between these theories has been developed: G. A. Baraff, Phys. Rev. **128**, 2507 (1962).
[5] B. N. Brockhouse ,Phys. Rev. Letters **2**, 256 (1959).

Being subject to both scattering mechanisms for most of their path, the electrons have an anisotropic distribution governed by the mean free path ratio $r=l_i/l_r$. During an ionization the primary electron loses an energy of at least the energy gap $\mathcal{E}_g$ and possibly considerably more for 4- to 5-eV electrons. An ionization collision will, therefore, reduce the chances of emission to zero for any but the most energetic electrons and will, therefore, be considered an absorption mechanism. For small values of r (ionization very probable) the phonon collisions, with relatively small energy losses, will have little opportunity to randomize the electron motion and a peak in the field direction will result. Larger values of r will give a more nearly spherical distribution under these circumstances.

The experiments were restricted to cases where the absorption by ionization is a valid assumption, either by an absolute upper cutoff on the distribution or by a distribution dropping off sufficiently fast to give negligible error. The distribution of emitted electrons was, therefore, made up of electrons which had suffered no ionizations in the spatial range of interest. The following qualitative analysis can be made of the scattering history of electrons released a known distance from the emitting surface in an energy range small compared with $\mathcal{E}_r$. The relative number that can escape with very few phonon collisions (small energy loss) is small since the probability of an electron traversing a distance of many mean free paths with few collisions is small. On the other hand, those electrons escaping with many phonon collisons (large energy loss) will have traveled a long random-walk-path length in reaching the surface. Their number will also be small because of the large probability of an absorptive ionization collision associated with the long path. The maximum escape probability occurs at an energy loss between these two limiting cases. The position of the peak will be a sensitive function of the ratio r, as will be the magnitude of the emitted distribution. We will return to a quantitative analysis of this behavior as applied to the actual experimental conditions.

The attenuation length measurement consisted of a measurement of the total number of electrons emitted as a function of the distance from the surface at which the electrons were released, not in a delta function as before, but in a Maxwellian distribution. The resulting increase in current with reduction of the intervening distance turns out to be relatively insensitive to r and provides an appropriate method of determining the magnitude of the mean free paths.

Experimental Conditions

The p-n junction electron emission structure described here differs from the devices used in other reported[6] electron emission observations, in that the

[6] J. A. Burton, Phys. Rev. **108**, 1342 (1957); J. Tauc, Nature **181**, 38 (1958); W. E. Spicer, Bull. Am. Phys. Soc. **5**, 69 (1960); B. Senitzky, Phys. Rev. **116**, 874 (1959).

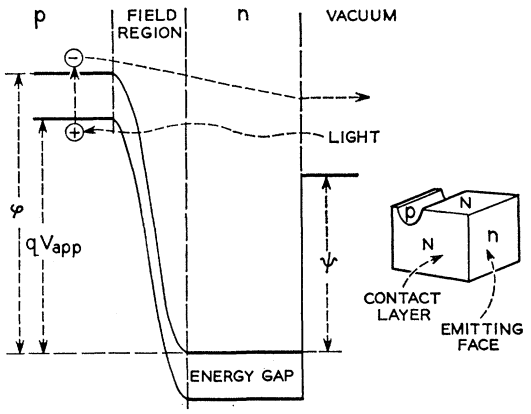

FIG. 1. Energy-band diagram and experimental structure. Two modes are possible: (1) Carriers created by light can be emitted from the p-type conduction band through the field and n regions, if they retain sufficient energy; (2) Carriers created in the junction at avalanche breakdown can be emitted if they are energetic enough.

junction was parallel to the emitting surface. The depth of the junction was 1300 Å, as determined by a method to be described.

Under reverse bias V_{app}, the band diagram (shown in Fig. 1) indicates the total potential energy drop across the junction for a conduction electron is

$$\varphi = qV_{app} + \mathcal{E}_g. \quad (1)$$

We have assumed that the Fermi level is at the band edges for the nearly degenerate material used. Emission of electrons can occur when electrons entering from the conduction band on the p-type side retain enough of their potential energy φ, after being swept across the junction to the surface, to overcome the electron affinity ψ. The advantage of this type of emission is that the problem is one dimensional, with all electrons exposed to the same basic history except for the scattering statistics. The surface from which they are emitted is, in principle, an equipotential so that a retarding potential measurement to analyze their energies is significant. The current of nonemitted electrons, however, must flow parallel to the surface to the n-type contact and a lateral voltage drop at high current will upset the equipotential to some extent.

Two modes of operation of the junction are possible. Electrons may be photoexcited in the p-type bulk. From there, some will diffuse toward the junction starting in the field region in an energy range (thermal energies) which is narrow compared to the final energy distribution at the emitting surface. The emitted distribution will have a peak at an energy dependent on r as described previously, provided the applied voltage is small enough that no electrons escape after suffering an ionization collision.[7] Fitting the shape and magnitude of this distribution will then determine r. An electron injecting p-n junction could serve a purpose similar to that of the light.

In the second mode of operation the junction was biased to breakdown and the emitted energy distribution was found to be nearly Maxwellian. With a Maxwellian distribution the diffusion of electrons from the n-type edge of the junction-depletion layer, which gives rise to an attenuation, can be related by a simple function to the dependence of the total emitted current on the thickness of the n layer. The attenuation length is related to the mean free paths, so that knowing the ratio r, l_i and l_r can be determined. The n layer was reduced in thickness in calibrated steps by oxidizing the surface in boiling water and removing the oxide with HF.

Relation Between Theory and Experiment

After this brief introduction to the experimental aspects of electron emission, we will turn to a more detailed mathematical analysis of an idealized model of the experimental structure. From this analysis we will determine the experimental conditions necessary for an understanding of hot-electron emission. The model as well as the actual structure can be divided into two regions (field and neutral n layer) and the surface potential barrier. In the next two sections the transport of hot electrons through the regions of this model will be related to the measurable features of the emitted electrons. Then, after a description of the experimental techniques in Sec. IV, the experimental results are interpreted by the adjustment of the fitting parameters l_i and l_r in Sec. V.

In Sec. II the junction will be treated as a constant field region into which electrons are injected in a nonsteady-state distribution. The initial transient behavior of the transport equation is, therefore, examined for a distribution with the position of its maximum sensitive to the value of r in the manner described earlier. One special case of this transient case is the injection and subsequent diffusion of electrons in a field-free (neutral) region. A second special case is the steady-state solution in a constant field region. Solutions to these two cases as well as the complete transient case are contained in the Appendix.

The solution to the differential equation governing the transient case will show that due to a necessary approximation a special group of electrons has been selected. This group consists of electrons that have had only a relatively small energy loss after their release in the junction and have as a result more than the average amount of kinetic energy. With their higher than average velocity these electrons represent the diffusive part of the solution. The solution with this diffusive nature allows us to treat the experimental problem of electrons released with zero energy at the start of the junction in terms of an idealized problem. It will be shown that, in spite of the very large field present, the electrons contributing to emission can be thought of as diffusing

[7] Clearly, with 5 V applied this is a justifiable assumption for a 3.8-eV electron affinity.

toward the surface after being released in a field-free region with an energy equal to the total potential across the junction. The inclusion of the neutral layer as an extension of the field region follows as a straightforward extension.

The energy distribution so obtained has the desired dependence on r. It must, however, be corrected for the reflection of the randomly oriented electrons by the surface potential barrier. An estimate of this effect is included in Sec. III.

The relation between the mean free paths l_i and l_r and the exponential decay in current with thickness of the neutral layer is calculated from simple diffusion theory for an incident Maxwellian distribution. The characteristic length is then a function of the ratio r and the electron temperature of the distribution as well as a parameter related to the magnitudes of l_i and l_r. The information obtained from fitting the experimental results with this characteristic length is then used in Sec. V to reduce the number of unknowns in the fit of the shape and magnitude of the photoexcited electron distribution to one, namely r.

II. ELECTRON TRANSPORT

The release of electrons with near zero energy in a field region, where a force $F=qE$ sweeps the electrons in the x direction, requires the transport equation to be examined for the initial transient behavior leading to the steady-state drift. Special cases of the equation are then the pure diffusion process for $F=0$ and the steady-state drift (independent of x).

The physical assumptions made here parallel very closely those made by Wolff. The details of the silicon band structure are ignored by using the free-electron model. Phonon scattering is assumed to be isotropic with a constant mean free path l_r and energy loss $\mathcal{E}_r$. Ionization will be characterized by the constant mean free path l_i and will be absorptive. The medium will be assumed to have an ionization threshold at zero energy since only near the beginning of the electron's path, starting from the p-type side in the photoexcited emission, will there be an error introduced. The l_i which results from this work represents an average mean free path over the energy range 0 to 5 eV weighted heavily towards the higher energy since the mean free path is expected to decrease with increasing energy and electrons are at high energies a majority of the time.

Certain combinations of l_i and l_r are convenient. In addition to $r=l_i/l_r$, we define the direct-flight mean free path l by

$$1/l=1/l_i+1/l_r, \tag{2}$$

and the diffusion attenuation length (or mean distance between collisions in the diffusion direction) λ, for absorptive ionization, by

$$\lambda^2=ll_i/3. \tag{3}$$

The time steady-state distribution function in momentum space is a function, by the assumed symmetry of the emission structure, of x, the magnitude of the momentum p, and the angle θ between x and $\mathbf{p}$. The number of electrons in the volume element $dV_p=2\pi p^2 \times\sin\theta d\theta dp$ is

$$N(x,p,\theta)=f(x,p,\theta)dV_p. \tag{4}$$

We will follow Wolff and assume a nearly spherical distribution which we will find to be reasonably justifiable in the range of greatest interest. We may then expand $f(x,p,\theta)$ in spherical harmonics and retain only the first two terms, if $f_0>f_1$. Thus,

$$f(x,p,\theta)\cong f_0(x,p)+f_1(x,p)\cos\theta. \tag{5}$$

The relationship between f_0 and f_1 which determines the justification for the retention of only two terms can be found in the energy range around the peak of the photoexcited emission distribution. We shall see later that near the peak in f_0

$$f_0/f_1=\lambda/l=[(1+r)/3]^{1/2}. \tag{6}$$

The condition $f_0>f_1$ will not be fulfilled over the entire range of interest for $r=3.2$. The violation of the condition will be illustrated quite graphically by the deviation between theory and experiment. The retention of only the first two terms, however, will prove to be better in this case than expected intuitively.

Solutions to the Transport Equation

Using the specific assumptions about the scattering mechanisms the transport equation is written in the Appendix as two coupled equations in f_0 and f_1. One of these provides a convenient relation between f_0 and f_1:

$$\frac{f_1(\varphi,\mathcal{E})}{lF}=-\frac{\partial f_0(\varphi,\mathcal{E})}{\partial\varphi}-\frac{\partial f_0(\varphi,\mathcal{E})}{\partial\mathcal{E}}, \tag{7}$$

where $\mathcal{E}=p^2/2m$ and $\varphi=Fx$ is the potential through which the electron has fallen at point x. If we define T as the energy lost by an electron to collisions in reaching the point x, i.e.,

$$T=\varphi-\mathcal{E}, \tag{8}$$

the transport equation can be written as a single partial differential equation in f_0. It can take two specific forms depending on whether φ and T or $\mathcal{E}$ and T are chosen as independent variables. The two special cases, steady state drift and diffusion, are then found from the limiting form of the suitable equation under the condition $\partial f_0/\partial x\rightarrow 0$ or $F\rightarrow 0$. The solutions to these equations are given in the Appendix and will be used where needed.

The solution to the complete equation is obtained in the Appendix as an approximation under the condition $2\mathcal{E}\gg r\mathcal{E}_r$. As noted earlier it represents a description of the diffusive nature of electrons in a drift field and can be used as a very good approximation for electrons with sufficient energy to escape over a barrier of height $\psi=3.8$ eV.

The solution

$$f_0(\varphi,T)=\frac{\text{const}}{T}\exp\left(-\frac{\varphi^2}{4\mathcal{E}_0 T}-\frac{T}{r\mathcal{E}_r}\right), \quad (9)$$

where

$$\mathcal{E}_0=F^2\lambda^2/r\mathcal{E}_r \quad (10)$$

can be converted to give $f_1(\varphi,T)$ using the appropriate form of Eq. (7). The flux of electrons traveling toward the surface, which is related to experimentally measurable currents, can be determined from $f_1(\varphi,T)$.

The nature of the solution can be examined if we plot the locus of the maximum of the f_0 distribution of Eq. (9) which occurs between $T=\varphi$ and $T=0$. Figure 2 shows this locus for the parameters of Wolff, Shockley, and the present work, using a field of 10^6 V/cm. We return to the discussion of Sec. I in which we mentioned that the peak of the distribution arose as a result of the increasing probability of transmitting an electron against phonon collisions with an increasing number of collisions (i.e., increasing T), counteracted by the increasing probability of absorption because of the increasing random-walk-path length. As ionization becomes relatively more probable, i.e., r becomes smaller, the peak shifts to a lower number of phonon collisions (smaller T) as shown by Fig. 2. Although the peak shifts to higher energies, the magnitude at the peak reduces rapidly with decreasing r. It is this position and magnitude dependence of the distribution maximum which can be fitted to the experimentally observed distribution to determine the value of r.

We have considered, in this section, solutions to three forms of the transport equation under much simplified conditions. We now turn to the application of these solutions (representing specific regions of the emission structure) to the two experiments of interest in order to obtain relations between measurable quantities.

III. APPLICATION TO SHALLOW JUNCTIONS

To be emitted, electrons must diffuse through the field-free n layer. Using the solution to the diffusion equation discussed earlier we can calculate the probability that an electron will penetrate this neutral layer with a certain energy loss. If the distribution impinging on the layer is Maxwellian, we may calculate the resulting distribution at the surface and its dependence on the thickness of the layer. For the peaked distribution, resulting from a delta function of photoexcited electrons entering the junction, we can show that to a good approximation the effect of the neutral layer on this distribution can be accounted for by extending the field region a distance equal to the neutral layer thickness.

Neutral Layer

The probability of transmission through the neutral layer is calculated from the flux of electrons

$$J(\mathcal{E})d\mathcal{E}=(8\pi m/3)\mathcal{E}f_1 d\mathcal{E}. \quad (11)$$

Equation (7) relating f_1 to f_0, for diffusion alone is

$$f_1=-l\partial f_0/\partial x, \quad (12)$$

so that we may write

$$J(T)dT=[\partial(\mathcal{E}f_0)/\partial x]dT,$$

where $\mathcal{E}f_0$ is the solution to the pure diffusion equation ($F=0$) treated in the Appendix [Eq. (A14)]. The probability that an electron entering the neutral layer at $x=0$ and $\mathcal{E}>T$ appears at $x=L$ in the energy range T to $T-dT$ is then, using appropriate normalization,

$$P_1(T,L)dT=J(T)|_{x=L}dT$$
$$=\frac{L}{2\lambda\sqrt{\pi}}\exp\left[-\frac{L^2}{4\lambda^2}\frac{r\mathcal{E}_r}{T}-\frac{T}{r\mathcal{E}_r}\right]\frac{dT}{T^{3/2}}. \quad (13)$$

The distribution at the emitting surface resulting from a Maxwellian distribution entering the neutral layer may be written as a function of the energy variable at the surface $\mathcal{E}_L=\mathcal{E}-T$, where $\mathcal{E}$ is the energy at which the electron enters, as

$$N(\mathcal{E}_L)=(2/\sqrt{\pi})(kT_e)^{-3/2}\int_0^\infty(\mathcal{E}_L+T)^{1/2}$$
$$\times\exp[-(\mathcal{E}_L+T)/kT_e]P_1(T,L)dT. \quad (14)$$

This integral can only be evaluated approximately. The integrand consists of a sharply peaked function times the factor $(\mathcal{E}_L+T)^{1/2}$, so that under certain conditions the integral may be written as the value of the integral without the factor $(\mathcal{E}_L+T)^{1/2}$ times this factor with T replaced by its value at the peak of the integrand. This procedure applied term by term to a Taylor series expansion of the square root leads to the following approximate expression under the conditions noted.

$$\int_0^\infty(1+gp)^\alpha\exp(-a^2p-b^2/p)\frac{dp}{p\sqrt{p}}$$
$$\cong\frac{\sqrt{\pi}}{b}e^{-2ab}\left(1+g\frac{b}{a}\right)^\alpha$$
$$\times\left[1+\frac{\alpha(\alpha-1)}{4ab}\left(1+\frac{a}{gb}\right)^{-2}+\cdots\right], \quad (15)$$

where $\alpha=\frac{1}{2}$ or $\frac{3}{2}$; $ga/b<1$; a^2, $b^2\gg1$.

The distribution at the surface is, therefore,

$$N(\mathcal{E}_L)=\frac{2}{\sqrt{\pi}}(kT_e)^{-3/2}\mathcal{E}_L^{1/2}$$
$$\times\exp(-\mathcal{E}_L/kT_e)e^{-L/L_0}\left(1+\frac{r\mathcal{E}_r}{\mathcal{E}_L}\frac{LL_0}{2\lambda^2}\right)^{1/2}$$
$$\times\left[1-\frac{L_0^2}{4L^2}\left(1+\frac{LL_0 r\mathcal{E}_r}{2\lambda^2\mathcal{E}_L}\right)^{-2}+\cdots\right], \quad (16)$$

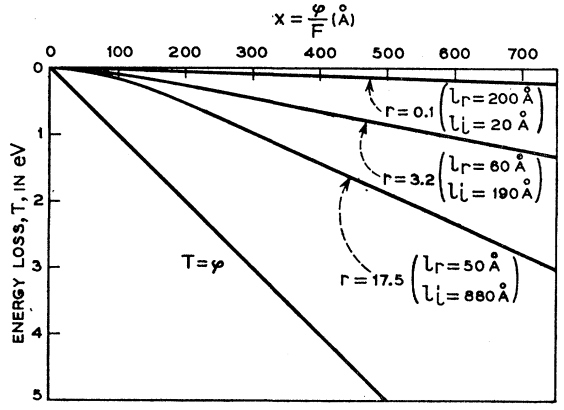

FIG. 2. The locus of the maximum of the density distribution of electrons released at position $x=0$ (start of the junction) for different values of $r=l_i/l_r$.

where

$$L_0^2=\lambda^2/(1+r\mathcal{E}_r/kT_e). \tag{17}$$

The values of the parameters L, L_0, and λ are such that the L dependence is governed to within 2% by $\exp(-L/L_0)$. We note that a Maxwellian distribution of the same temperature as that which entered, reduced in magnitude by $\exp(-L/L_0)$, appears at the surface. The experimental procedure, therefore, consists of measuring this L dependence in a situation where a Maxwellian distribution is observed externally. The electron emission due to avalance breakdown meets these requirements. The reflection of electrons at the surface will not affect the attenuation measurement as long as it remains constant during the experiment.

Field Region

Before attempting to repeat a calculation of this type for the distribution of photoexcited carriers, it is necessary to establish the method by which the magnitude of this distribution can be obtained from the retarding potential experiment. Clearly the derivative with respect to energy of the emitted electron current measured as a function of the collector potential in retarding potential measurement, normalized by the photocurrent incident on the junction from the p-type side, corresponds to the probability that an electron starting at the conduction band edge traverses the junction and neutral layer, overcomes the surface barrier, and is emitted in the appropriate energy range. We will, therefore, calculate a probability analogous to $P_1(T,L)$ for the field region, integrate it with $P_1(T,L)$, and then multiply it by the appropriate reflection factor.

We note that for the independent variables φ and T Eq. (7) becomes

$$f_1/lF=-\partial f_0(\varphi,T)/\partial\varphi. \tag{18}$$

The probability of transmission through the field region can, therefore, be found from Eq. (9):

$$P_2(\varphi,T)dT=\frac{1}{4\mathcal{E}_0}\left(\frac{\varphi^2}{T^2}-\frac{\varphi}{T}\right)\times\exp\left[-\frac{x^2}{4\lambda^2}\frac{r\mathcal{E}_r}{T}-\frac{T}{r\mathcal{E}_r}\right]dT. \tag{19}$$

We have used both φ and x in this expression to bring out the similarity of the exponential term to that of Eq. (13). φ and x are now considered the total applied potential energy and the width of the junction, respectively. The normalization to a unit delta function was carried out in the limit $\varphi\rightarrow 0$ because of the approximate nature of the solution given in Eq. (9).

We now define

$$U=\varphi-\mathcal{E}_L \tag{20}$$

to be the over-all energy loss of an electron traversing the field region and the neutral layer, so that the over-all transmission to the surface is given by

$$P(x,L,U)=\int_0^U P_2(\varphi,T)P_1(L,U-T)dT \cong\frac{1}{4\mathcal{E}_0}\left\{\left[\frac{\varphi(1+L/x)}{U}\right]^2-\frac{\varphi(1+L/x)}{U}\right\}\times\exp\left[\frac{(x+L)^2}{4\lambda^2}\frac{r\mathcal{E}_r}{U}-\frac{U}{r\mathcal{E}_r}\right]\quad(\text{for } L<x), \tag{21}$$

where we substituted $U-T$ for T in Eq. (13) and used the integral of Eq. (15) for $\alpha=\frac{1}{2}$ and $\frac{3}{2}$ to obtain the approximate result. The approximation is accurate to 4% in the application to the experimental results.

The form of Eq. (21) is identical to that of Eq. (19) with $x+L$ substituted for x. We, therefore, define

$$X=x+L$$

and

$$\Phi=FX=\varphi(1+L/x). \tag{22}$$

This result suggests that the whole effect of diffusion through the neutral layer may be included by considering a field region increased in width by L. This diffusion nature of the field region solution deemphasizes the importance of the exact field distribution (under the condition $2\mathcal{E}\gg r\mathcal{E}_r$), so that the theory based on a constant field in the junction can be applied to the structure in which, as we shall see, the field is quite nonuniform. At the start of the junction the electrons will be affected by the field, but since at that point they are below the ionization threshold, where the theory does not apply, we can consider X to be a fitting parameter whose value is variable in a range determined by the actual junction width.

Relation to Experiment

We define $K(\mathcal{E}_L)$ to be the percentage of electrons transmitted over the surface potential barrier, after

being incident on the barrier with energy $\mathcal{E}_L$, as a result of being transmitted to the surface by the probability $P(x,L,U)$. Then if I_0 is the current of photoexcited electrons entering the junction and $I_{\rm em}(U)$ is the current collected externally as a function of a retarding potential, the emitted electron energy distribution is given by

$$\beta(U)dU\equiv\frac{1}{I_0}\frac{dI_{\rm em}(U)}{dU}dU \tag{23}$$

$$=K(\varphi-U)\frac{1}{4\mathcal{E}_0}\left(\frac{\Phi^2}{U^2}-\frac{\Phi}{U}\right)\times\exp\left[-\frac{X^2}{4\lambda^2}\frac{r\mathcal{E}_r}{U}-\frac{U}{r\mathcal{E}_r}\right]dU. \tag{24}$$

In obtaining the expression following $K(\varphi-U)$ we have assumed that all those electrons with energies greater than the barrier are emitted. Those reflected by the barrier because of their transverse momentum can be accounted for separately in the absence of electron-electron collisions. We will establish limits on the magnitude of $K(\mathcal{E}_L)$, the lower given by allowing electrons only one attempt to escape, the upper by considering the electrons free to be randomly reflected by lossless phonon collisions, but limited in the number of escape attempts by ionization absorption. In addition to electrons directed toward the surface given by the flux $P(x,L,U)$, there are those due to the accompanying density distribution which can also be emitted. We need, therefore, the ratio f_0/f_1, and may at the same time investigate the applicability of the expansion of f in terms of spherical harmonics.

For the distribution function f_0 as given by Eq. (9), the ratio f_1/f_0 is obtained from Eq. (18) as

$$f_1/f_0=(lF/2\mathcal{E}_0)\varphi/T. \tag{25}$$

Substitution of FX for φ and U for T gives the value of f_1/f_0 at the emitting surface, with the result that

$$f_1/f_0=3X\mathcal{E}_r/2l_rU \text{ (at the surface)}. \tag{26}$$

The distribution f_0 has a maximum which occurs at $\varphi/T=(1+r\mathcal{E}_r/T)^{1/2}2F\lambda/r\mathcal{E}_r$. Thus, for $T\gg r\mathcal{E}_r$ we obtain at the maximum of f_0

$$f_1/f_0=l/\lambda=[3/(1+r)]^{1/2} \text{ (at the maximum of } f_0). \tag{27}$$

Using the experimental values, Eq. (27) gives a reasonable justification for the expansion in spherical harmonics, but because the maxima of f_1 and f_0 do not coincide Eq. (26) gives an f_1 smaller than f_0 through only part of the energy range in which the experimental data are fitted. We shall return to a fuller discussion of this point and assume for the present that in the range of interest f_1 and f_0 are comparable.

Surface Reflections

The electrons with energy $\mathcal{E}_L$ which escape in the first attempt are all those with a direction of momentum in a cone of angle θ_0 given by

$$\cos\theta_0=(\psi/\mathcal{E}_L)^{1/2}=\mu. \tag{28}$$

The number of electrons escaping on the first attempt at an energy $\mathcal{E}_L$, normalized to those incident, is therefore

$$\int_0^{\theta_0}(f_0+f_1\cos\theta)dV_p\Big/\int_0^{\pi/2}(f_0+f_1\cos\theta)dV_p=f_0(1-\mu)+f_1(1-\mu^2). \tag{29}$$

The lower limit on $K(\mathcal{E}_L)$ is, therefore,

$$K_0(\mathcal{E}_L)=(1+f_0/f_1+\mu)(1-\mu). \tag{30}$$

The upper limit may be estimated by considering phonon collisions to be lossless randomizing collisions, which return electrons to the surface after each reflection until they are emitted, absorbed by ionizations, or until they have suffered a number of phonon collisions

$$n=(\mathcal{E}_L-\psi)/\mathcal{E}_r, \tag{31}$$

and they have insufficient energy for escape. We have, thus, overestimated the escape probability by neglecting the reduction in critical angle θ_0 with energy loss and all single- or multiple-phonon processes which prevent the electron from returning to the surface. The upper limit $K_r(\mathcal{E}_L)$, resulting from the sum of a finite series of tries, is determined for r near 1 by the ionization absorption process. We find

$$K_r(\mathcal{E}_L)=(r+1)[1+r(1-\mu)]^{-1}\{K_0-(1-\mu)\mu r/(r+1)-[K_0-(1-\mu)][\mu r/(r+1)]^n\}. \tag{32}$$

For $n\gg1$ the term containing the n becomes negligible, i.e., electrons are absorbed by ionization before dropping below ψ if they start with a large enough energy. We note that $K_{r=0}(\mathcal{E}_L)=K_0(\mathcal{E}_L)$. To show the energy dependence of $K(\mathcal{E}_L)$, $K_r(\mathcal{E}_L)(1+f_0/f_1)^{-1}$ is plotted in Fig. 3 for several values of r. We note that the energy dependence of $K_{3.2}(\mathcal{E}_L)$ does not differ greatly from $K_0(\mathcal{E}_L)$ over the range of interest except for a multiplicative factor. At low energies ($n<6$) the effect of the finite series is evident for $K_r(\mathcal{E}_L)$ for which the infinite series approximation is shown by the dashed curve. The dependence of f_0/f_1 on r, given by Eq. (27), was used for these curves.

We note that in correcting the Maxwellian distribution for surface reflections, the reflection theory for a spherical distribution, f_0, was used in the lower limit only, i.e.,

$$K_0'(\mathcal{E}_L)=1-\mu. \tag{33}$$

IV. DEVICES AND PROCEDURES

The particular geometry of the emission structure was chosen because of its over-all small size which allows a favorable retarding potential geometry. An emitting p-n junction was diffused into 0.02 Ω-cm p-type silicon, over an area of 0.050 in. on a side. This area was one face of a

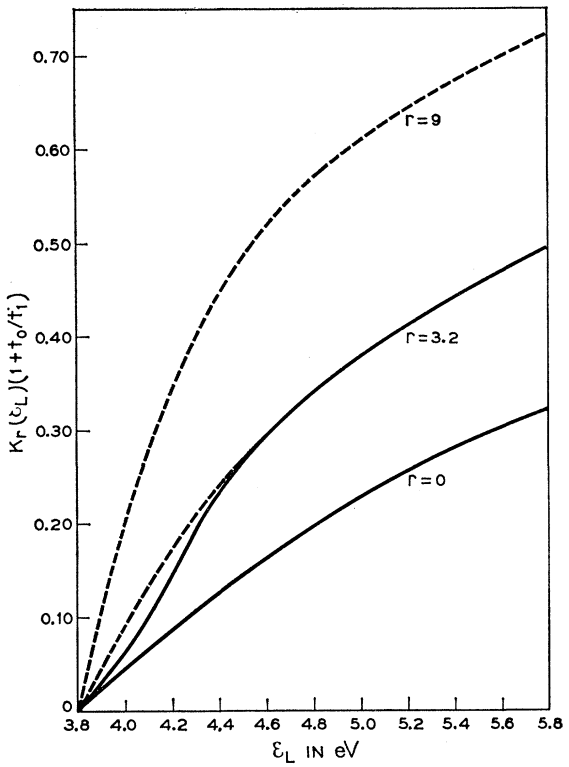

FIG. 3. The surface reflection factor for a 3.8-eV energy barrier for different values of r. $K_0(\mathcal{E}_L)$ is considered a lower limit on the number of electrons transmitted over the barrier while curves for higher values of r give $K_r(\mathcal{E}_L)$ as an upper limit.

cube, the other faces of which were previously diffused to give high-breakdown (10 V) contact junctions, such that the emitting junction diffusion made contact to them. Contact to the p-type bulk was made through a slot cut in one of the contact faces (see Fig. 1).

The emitting face was diffused for 14 min at 880°C with P_2O_5 in an open boat. Breakdown occurred between 5 and 6 V, the range of simultaneous tunnel and avalanche breakdown in silicon. The details of the shallow junction diffusion, such as the depth of the junction below the surface and the concentration gradient, were determined on a somewhat larger test cube by sectioning the n-type layer. The conductivity was measured through four of the n-layer (n) sides between contacts made to two thick n-layer (N) faces as shown in Fig. 4(a). Material was removed from the test cube by oxidizing the silicon in boiling water for 1 min and removing the oxide in HF. The amount of silicon removed by this boiling water-HF (BW-HF) method was determined from the weight loss with repeated cycles, as measured on a Mettler Micro-Gramatic balance. The oxide growth saturates after 1 min and the removal rate is nearly independent of the concentration of uniformly doped material. On samples such as the test cubes containing a shallow junction, however, the removal rate dropped to about 5 Å/cycle, from the otherwise constant rate of 33 Å/cycle, when less than 600 Å remained between the junction and the surface [Curve A, Fig. 4(b)]. Forward biasing the junction with light allowed the removal rate to be partially (Curve B) or completely (Curve C) restored to the bulk rate and could even be made to exceed it with sufficient light intensity. The removal rate, however, returned to nearly 33 Å/cycle when the junction was reached, independent of the light intensity (Curve B). A carrier injection model may explain this phenomenon in view of the junction bias dependence and the abrupt change in rate at the junction.

The diffusion profile calculated from the conductivity measurement is shown also in Fig. 4(a). The characteristic "flat top" near the surface is noted, as is the nearly constant gradient of 1.0×10^{25} cm^{-4} beyond it. The charge and field distributions (at 5 V applied) shown result from an extension of the linear gradient and the approximation of uniform positive charge on the p-type side. The peak field of 2×10^6 V/cm at 5 V indicates

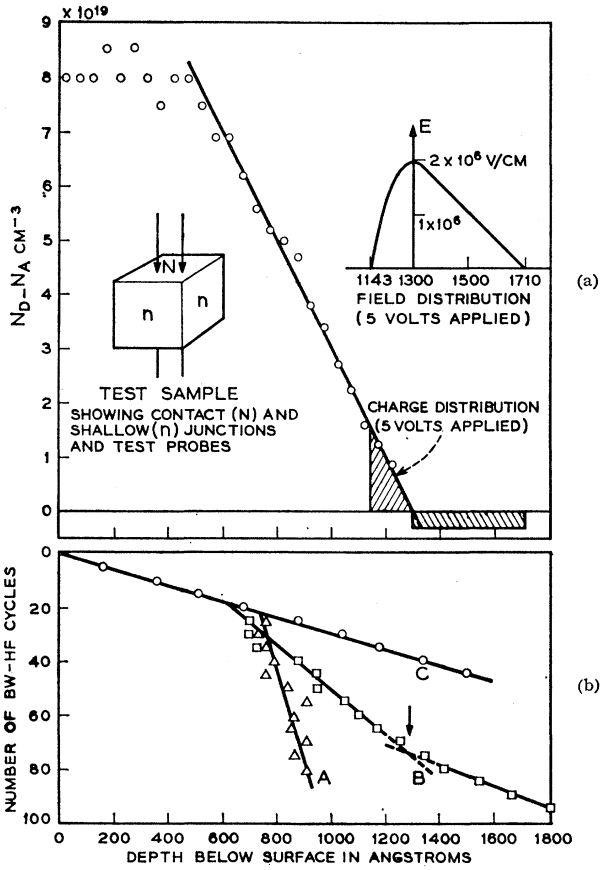

FIG. 4. (a) Diffusion profile obtained by sectioning the n-layer of a test sample with the boiling water-HF (BW-HF) method. Also shown are the charge distribution assumed (note the approximation of uniform charge on p-side) and the resulting field distribution. (b) Calibration of BW-HF method for samples containing shallow junctions. Curves A, B, and C correspond to zero, and two different amounts of light applied to the test sample during the boiling part of the cycle. Curve C was used to obtain the results shown in (a).

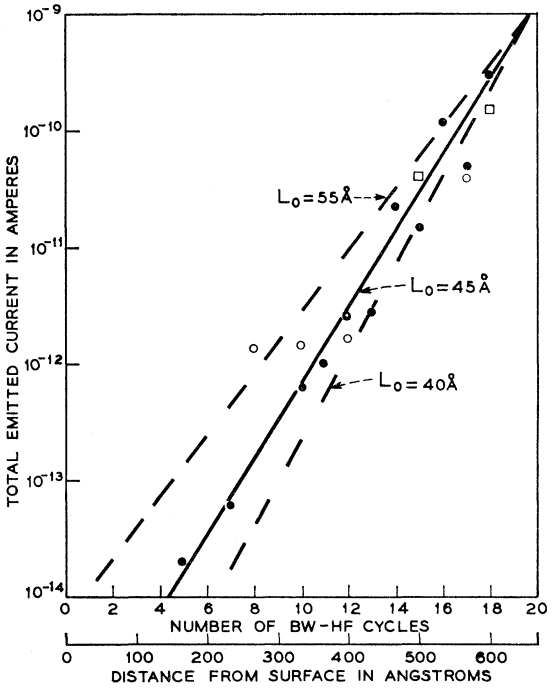

FIG. 5. Variation of the total emitted current with thickness of the neutral layer.

that at least part of the breakdown current is due to tunneling.

The BW-HF method gives a uniform removal rate of 33 Å/cycle over the first 700 Å of the n layer. It was, therefore, used within this range only for measurements of the dependence of the emitted current on the neutral layer thickness.

Of utmost importance to the magnitude of the emitted current is the cleanliness of the surface of the sample. Particularly any oxide, such as that grown in air at room temperature, must be removed to obtain consistent current measurements because electrons would have to tunnel through the thin potential barrier. The native oxide can be removed by etching with HF gas such as that liberated by decomposing ammonium bifluoride at 150–200°C. A thin-walled heater tube containing a few small crystals of ammonium bifluoride was positioned with the only opening facing the sample and heated electrically while the device was kept approximately 50°C hotter to avoid contamination by the ammonium fluoride byproducts.

A second method of avoiding oxide contamination consisted of protecting a freshly HF dipped sample from air during mounting and subsequent pumping of the vacuum system, by means of methyl alcohol. The alcohol has a slight reducing effect on silicon that appears to persist momentarily, even after it evaporates. Improvements in the emission current over oxidized surfaces by these methods ranged from a factor of 20 to 500.

The emitted electron current was collected on a hemispherical gold collector in which a small hole allowed light to pass to the emitting surface. A small positive spherical grid was used during the retarding potential measurements to accelerate the electrons radially so that their total energy rather than that normal to the surface was measured. The maximum sensitivity of the ammeter was 10^{-14} A.

V. EXPERIMENTAL RESULTS AND INTERPRETATION

Attenuation Length

The variation of the total emitted current with the thickness of the neutral layer is shown in Fig. 5 for several devices with a constant breakdown current of 25 mA. The exponential increase in current, with $L_0=45$ Å, is drawn through the points obtained from the best device. The remaining data adds support by virtue of having the same absolute magnitude. On some devices (data not shown) a similar slope was observed but with an apparent shift to the left indicating that some of the silicon was removed during the initial cleaning step (due perhaps to foreign material on the surface). The limits which can be put on L_0 from the data shown and general experimental conditions will be taken to be

$$L_0=45^{+10}_{-5}\text{ Å}. \tag{34}$$

The energy distribution for breakdown electrons, as measured from the emitted distribution, and corrected

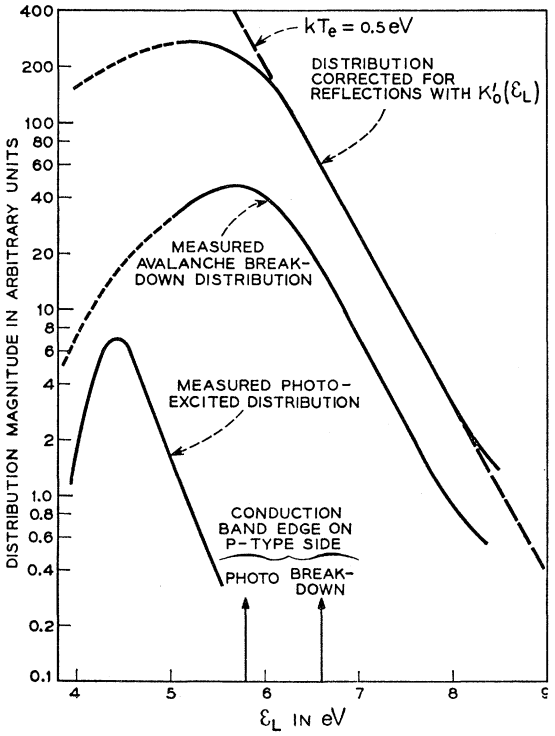

FIG. 6. Shape of the emitted photoexcited and avalanche breakdown energy distributions and the avalanche distribution corrected for surface reflections.

for surface reflections is shown in Fig. 6. The resulting distribution is Maxwellian over about two decades in the high-energy tail with a temperature

$$kT_e = 0.5 \pm 0.1 \text{ eV}, \tag{35}$$

but shows a significant deviation at lower energies. This deviation is probably due to the nonuniform surface potential resulting from the lateral voltage drop in the thin layer due to the large (25-mA) breakdown current. The potential barrier in the center of the emitting face is then effectively somewhat higher, an effect which is reduced, though not eliminated for distributions measured with thicker layers.

An important feature of the emitted distribution is the presence of electrons more energetic than those at the conduction band edge on the p-type side as calculated from the 5.5 V applied (see Fig. 6). The mechanism for the generation of such hot electrons can be one of two types consistent with conservation of energy.

The breakdown current due to avalanche multiplication flowed in microplasmas, as was observed from the recombination radiation. Electron densities in a microplasma are quite high, typically 10^{16}–10^{17} cm^{-3}, and electron-electron collisions under these circumstances may thermalize the distribution. Stratton[8] has proposed a criterion for the density at which the distribution becomes Maxwellian and his criterion gives a density in the above range for the electron temperature of 0.5 eV.

The second possible mechanism by which electrons can attain energies in excess of the p-type conduction band edge involves the actual avalanche multiplication. A few electrons will traverse such a large portion of the junction, before their first ionization collision, that they have energy considerably in excess of that needed for the secondary generation. If this energy is given up to the hole formed and the hole is also sufficiently fortunate in achieving a large amount of energy which is then given to the secondary electron it produces, electrons may gain energy from the field upon successive traversings of the junction. No estimate of the magnitude of the effect has been given.

The measured electron temperature may be compared with the theoretical expression (not applicable in case of electron-electron collisions) given by Eq. (A15), but an appropriate average field must be chosen. Using an average field estimated from Fig. 4 at 10^6 V/cm and the parameters quoted in the introduction, we find a temperature of 0.45 eV from the electron emission parameters, in good (perhaps fortuitous) agreement with experiment, and the values of 0.11 eV and 0.73 eV for Wolff's and Shockley's parameters, respectively. With a nearly linear field dependence and no accurate way of determining the average field, the significance of these figures is quite limited.

The value of L_0 can also be shown to be consistent with an extrapolation of the total emitted current to the edge of the depletion layer. An estimate of the number of electrons emitted over a 3.8-eV barrier, due to a 25-mA current at the junction edge, using a distribution as described by Wolff (with $\mathcal{E}_i = 1.8$ eV) and a simple spherical distribution reflection correction, requires a value of $L_0 = 46$ Å to fit the magnitude of the observed emission. The conversion from electron flux to density which tends to decrease L_0 and the effect of the nonuniform surface potential which would increase L_0 have been neglected in the estimate.

[8] R. Stratton, Phys. Rev. **126**, 2002 (1962).

Photoexcited Distribution

The retarding potential measurement of the photoexcited electron emission at a junction voltage below breakdown is also shown in Fig. 6, with the p-type conduction band edge shown for reference. The position of the peak of this distribution is much closer to the top of the surface potential barrier than the breakdown distribution. The temperature of the upper tail is lower, only 0.3 eV (a change not commensurate with the slight decrease in the junction field with 0.8 V lower bias), which, together with the surface reflections and the varying surface potential, would give rise to a lower energy peak, even for a Maxwellian distribution. However, several factors indicative of a fundamentally different distribution may be cited. The photocurrent was only 1 mA and the lateral voltage drop was correspondingly lower. We also note that the transmission factor for classical surface reflections is a relatively slowly varying function (within the limits discussed earlier) and could not by itself give rise to the observed peak. Furthermore, the position of the peak relative to the band edge indicates that the nature of this distribution is different than that for breakdown electrons. The reservation which remains in order is the uncertainty in the complete reflection factor, including quantum mechanical reflections.

The fit of the theoretical curve to the data proceeds as follows: The magnitude of $\beta(U)$ of Eq. (23) was determined from the photocurrent and the retarding potential data and the data were smoothed as shown in Fig. 7. From this magnitude ($\sim 10^{-8}$ eV^{-1}) and an estimate of the linear terms of Eq. (24), we find a magnitude for the exponent of this expression at a particular value of U ($=1$ eV). We now replace λ in this relation by the experimental values of L_0 and kT_e using Eq. (17). With all energies expressed in eV, we then have

$$\left(\frac{X}{2L_0}\right)^2 \frac{1}{1/r\mathcal{E}_r + 2} + \frac{1}{r\mathcal{E}_r} = 19.3. \tag{36}$$

The choice of $X/2L_0$ will then determine r. X may be obtained from the field distribution (shown in Fig. 4) and length L, which is determined by the amount of silicon removed at the time of the measurement. With 21 BW-HF cycles $X = 1010$ Å at the applied bias. We noted earlier that the constant field approximation in

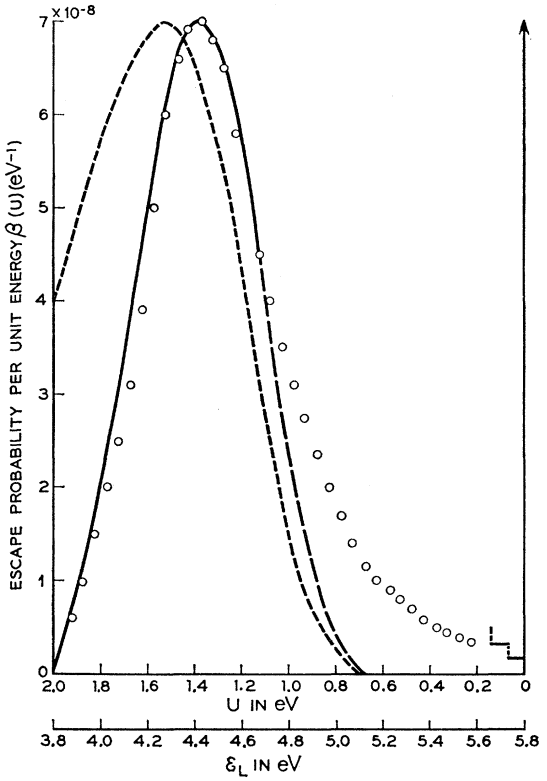

FIG. 7. Fit of the shape of the emitted energy distribution of photoexcited electrons with a theoretical curve (solid line) using parameters determined from the magnitude of the observed distribution. Adjustment of 0.1 eV was made in the relative scales of U (the energy loss in traversing the junction and neutral layer) and $\mathcal{E}_L$ (the kinetic energy at the surface). The two steps near $U=0$ are a magnitude calculation of the number of electrons emitted in an energy range $\mathcal{E}_r$ for electrons with zero and one collision, using the same parameters. The dashed curve corresponds to the calculated distribution without the effect of surface reflection (arbitrary scale).

the junction is valid only for the region where the electrons of interest are energetic enough to diffuse rather than drift. At low energies this assumption is no longer valid and the situation is further complicated by the fact that the initial portion of the electrons trajectory is below the ionization threshold. Clearly the X to be used here should be somewhat less than the 1010 Å, but how much less is uncertain.

Choosing $X/2L_0=10$ as a reasonable value, we obtain $r\mathcal{E}_r=0.2$ eV from which $r=3.2$. The solid curve in Fig. 7 shows the shape calculated from Eq. (24) using $r=3.2$ and the reflection factor $K_0(\mathcal{E}_L)$. The factor $K_{3.2}(\mathcal{E}_L)$ changes the shape by only a few percent and actually improves the fit in the range where the theory is applicable. The effect of the reflections on the position of the maximum is relatively small as can be seen from the dashed curve, which corresponds to the calculated distribution before emission over the barrier, plotted on an arbitrary scale.

One adjustment, other than the choice of $X/2L_0$, was a 0.1-eV shift in the relative energy scales, U and $\mathcal{E}_L$. From the junction voltage and the energy gap, φ was placed at 5.9 eV (the uncertainty due to contact resistance and perhaps lateral voltage drop across the emitting face is ± 0.1 eV). The initial rise of the distribution with increasing energy and the electron affinity of the gold collector place the electron affinity at $\psi=3.8$ eV. The relation between U and $\mathcal{E}_L$ used to obtain the best fit, corresponds by Eq. (20) to a value of $\varphi=5.8$ eV. This may be interpreted as either the limit of the error range on φ, or the need for an electron affinity $\psi=3.9$ eV.

Before discussing the deviation of theory and experiment in the energy range above the maximum, we will investigate the sensitivity of the position of the peak to changes in r, X, and L_0. If we vary r by ± 1, the theoretical peak shifts by ∓ 0.3 eV. This value is not unrealistic as the limit of accuracy of the measurement. Keeping the magnitude of the distribution constant this range of r corresponds, according to Eq. (36), to a variation in $X/2L_0$ from 9.5 to 10.5. At this point we may include the range of uncertainty of X and compare the required extremes in L_0 with those obtained from the direct measurement. We obtain

$$\left.\begin{aligned} &L_0\sim 45-55 \text{ Å}; r=4.2\\ &L_0\sim 40-50 \text{ Å}; r=2.2\end{aligned}\right\} 850 \text{ Å}<X<1050 \text{ Å}. \quad (37)$$

The compatability of this uncertainty with that obtained earlier indicates a degree of self-consistency.

Using $r=3.2$ and $L_0=45$ Å, Eq. (17) gives the value $\lambda=53$ Å for the electron temperature observed. From the definition of $\lambda\,[=(ll_i/3)^{1/2}]$ we obtain $l_r=60$ Å and $l_i=190$ Å. Figure 8 shows the relationship between these values and those used by Wolff and by Shockley. Also shown are the self-consistent extremes calculated from the two experiments.

The deviation between theory and experiment at energies above the peak can be attributed to a breakdown of the applicability of the theory. The expansion of f in terms of spherical harmonics is valid only for $f_0>f_1$. As long as the coefficients f_n are decreasing for increasing n, the flux, representing all particles moving in the x direction, will very nearly be described by Eq. (11). The integral over the hemisphere centered on the x axis vanishes or is very small for all higher order spherical harmonics. The condition giving the breakdown of the theory is, therefore, $f_0\cong f_1$, which according to Eq. (26) occurs at approximately the peak of the distribution of Fig. 7. For smaller U the distribution is then more sharply peaked in the forward direction until at $U=0$ electrons with no collisions will represent a very sharp forward spike. Since at the field region start the direction of electrons can easily be changed to the x direction, independent of the initial direction, electrons with zero collisions are not affected by surface reflections. Hence, $\beta(U)dU$ at $U=0$ is given by

$$\beta(0)=e^{-X/l}(1/\mathcal{E}_r)\text{ eV}^{-1}. \quad (38)$$

Using $X=1010$ Å and $l=45$ Å determined from l_i and l_r by Eq. (2), we find a magnitude 1.75×10^{-9} eV^{-1}, which is shown in Fig. 7 as a small line at $U=0$. The $\mathcal{E}_r$ appears to define the energy range in which the electrons emerge, ionization being absorptive.

The number of electrons escaping with only one collision can be written as the probability that the collision was not an ionization $[r/(r+1)]$, times the integral, over all angles and positions, of the probability of avoiding a collision before and after the single collision. Again we assume the electron enters the field region normal to the surface, so that

$$\beta(\mathcal{E}_r)=\frac{1}{\mathcal{E}_r}\frac{r}{r+1}\int_0^{\pi/2}\int_0^X e^{-x/l}\frac{dx}{l}\exp\left(-\frac{X-x}{l\cos\theta}\right)\sin\theta d\theta$$

$$=\frac{1}{\mathcal{E}_r}\frac{r}{r+1}\left[e^{-X/l}\left(\ln\frac{\gamma X}{l}-1\right)+E_{n=1}\left(\frac{X}{l}\right)+E_{n=2}\left(\frac{X}{l}\right)\right], \quad (39)$$

where $\gamma=1.781$ and E_n is the exponential integral. The asymptotic form of E_n then gives, for large X/l,

$$\beta(\mathcal{E}_r)=\beta(0)\frac{r}{r+1}\left(\ln\frac{\gamma X}{l}-1+\frac{2l}{X}\right). \quad (40)$$

The second step near $U=0$ in Fig. 7 results. The resulting slope and magnitude are in good agreement with the observed distribution.

One further theoretical difficulty which is not apparent here is the breakdown of the description of the statistical scattering process by means of a differential equation when only a few collisions are involved. Since at the peak about 20 phonon collisions have occurred, no difficulty arises in the range of applicable theory.

VI. CONCLUSION

The characteristics of the emission of hot electrons from shallow junctions in silicon can be explained quantitatively by a theory using mean free path parameters intermediate to the values used by Wolff and Shockley. The fit to the data is good, perhaps fortuitous considering the rather drastic assumptions regarding band structure, constancy of the mean free path, details of uniformity of the layer, and cleanliness of the surface.

Again we emphasize that the observed peak in the distribution may be the result of a more strongly energy-dependent surface barrier reflection phenomenon than that described by the simple theory.

ACKNOWLEDGMENTS

The authors wish to thank U. Sorenson and R. Taperall for preparing the samples and S. Sze for making the weight-loss measurements.

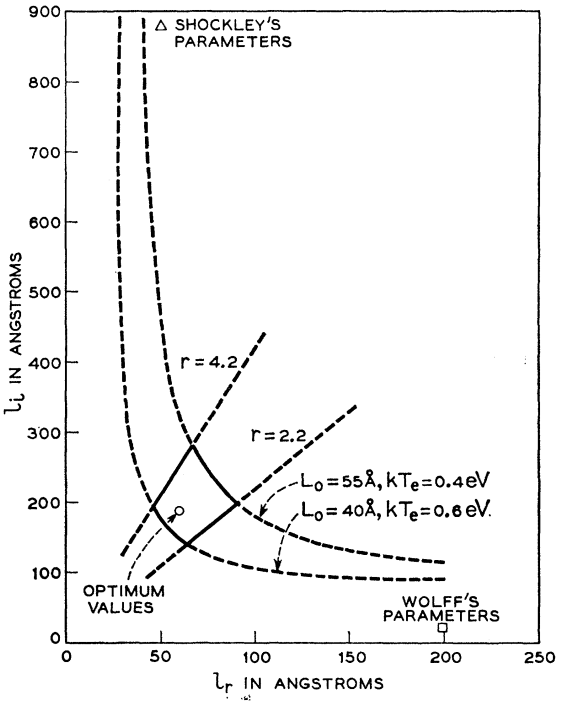

FIG. 8. The relation between the parameters of Wolff and Shockley, and the optimum point. Also shown is the self-consistent range of parameters (solid line) and the relations imposed by the two separate experiments (dashed lines).

APPENDIX: SOLUTIONS TO THE TRANSPORT EQUATION

The transport equation is written for a region where scattering by phonons is isotropic, ionization is absorptive, and the mean free paths are constant. The second-order partial differential equation which results is then solved for the case of pure diffusion, steady-state drift, and the more complete transient case where both drift and diffusion are important.

Collision Terms

To obtain the phonon and ionization collision terms in the transport equation we consider an infinitesimally thin ring of volume dV_p at angle θ and calculate the net rate of electrons entering and leaving. All electrons entering the ring start with the same momemtum p' determined by conservation of energy. Assuming isotropic scattering electrons scattered from a spherical shell at p' are distributed uniformly over the shell at p. The contribution of the electrons entering the ring is then the average number leaving the p' shell, corrected by the ratio of the volumes of the two shells. Hence,

$$\left.\frac{\partial f}{\partial t}\right|_{\text{phonons}}=-\frac{v}{l_r}\left\{f_0(x,p)+f_1(x,p)\cos\theta\right\}+\frac{v'}{l_r}f_0(x,p')\frac{p'^2dp'}{p^2dp}, \quad (A1)$$

where v and v' are the velocities corresponding to p and p' and the $f_1(x,p')$ contribution from the entering electrons vanishes by the orthogonality of the spherical harmonics. From conservation of energy in a phonon collision and the small magnitude of $\mathcal{E}_r$ compared with the kinetic energy of the several electron-volt electrons of interest, we obtain

$$p'-p\cong m\mathcal{E}_r/p\ll p.$$

We may, therefore, expand $f_0(x,p')$ about p and retain only the first two terms as an approximation. By neglecting terms in $\mathcal{E}_r^2$ this procedure results in

$$\left.\frac{\partial f}{\partial t}\right|_{\text{phonons}}=v\left(-\frac{f_1\cos\theta}{l_r}+\frac{\mathcal{E}_r}{l_r}\frac{1}{\mathcal{E}}\frac{\partial\mathcal{E}f_0}{\partial\mathcal{E}}\right), \quad \text{(A2)}$$

where $\mathcal{E}=p^2/2m$. Since ionization is assumed to be absorptive, we write

$$\left.\frac{\partial f}{\partial t}\right|_{\text{ioniz}}=v\left(-\frac{f_0}{l_i}-\frac{f_1\cos\theta}{l_i}\right). \quad \text{(A3)}$$

Transport Equation

The transport equation,

$$\left.\frac{\partial f}{\partial t}\right|_{\text{phonons}}+\left.\frac{\partial f}{\partial t}\right|_{\text{ioniz}}=v\cos\theta\frac{\partial f}{\partial x}+F\frac{\partial f}{\partial p_x}$$
$$=v\cos\theta\left(\frac{\partial f}{\partial x}+F\frac{\partial f}{\partial\mathcal{E}}\right)-v\frac{\sin\theta}{2\mathcal{E}}\frac{\partial f}{\partial\theta}, \quad \text{(A4)}$$

can be written in terms of the assumed angular dependence as

$$\frac{\mathcal{E}_r}{l_r}\frac{1}{\mathcal{E}}\frac{\partial(\mathcal{E}f_0)}{\partial\mathcal{E}}-\frac{f_0}{l_i}-\frac{Ff_1}{2\mathcal{E}}-\cos^2\theta\left[F\left(\frac{\partial f_1}{\partial\mathcal{E}}-\frac{f_1}{2\mathcal{E}}\right)+\frac{\partial f_1}{\partial x}\right]$$
$$=\cos\theta\left(\frac{f_1}{l_r}+\frac{f_1}{l_i}+\frac{\partial f_0}{\partial x}+F\frac{\partial f_0}{\partial\mathcal{E}}\right). \quad \text{(A5)}$$

Multiplication by $\sin\theta\cos\theta d\theta$, or $\sin\theta d\theta$ and integration from $\theta=0$ to π causes, respectively, the left- or the right-hand side to vanish identically, so that

$$\frac{f_1}{lF}=-\frac{\partial f_0}{\partial\varphi}-\frac{\partial f_0}{\partial\mathcal{E}}, \quad \text{(A6)}$$

and

$$\frac{1}{\mathcal{E}_0}\frac{\partial(\mathcal{E}f_0)}{\partial\mathcal{E}}-\frac{\mathcal{E}f_0}{F^2\lambda^2}=\frac{\partial}{\partial\varphi}\left(\frac{\mathcal{E}f_1}{lF}\right)+\frac{\partial}{\partial\mathcal{E}}\left(\frac{\mathcal{E}f_1}{lF}\right), \quad \text{(A7)}$$

where

$$\mathcal{E}_0=F^2\lambda^2/r\mathcal{E}_r \quad \text{(A8)}$$

is the steady-state electron temperature which could be obtained from elementary energy balance considerations. $\varphi=Fx$ is the potential energy gained by the electron and corresponds to the potential drop across the junction when x is the junction width under a constant field approximation. Here φ will be considered variable. Using the definition

$$T=\varphi-\mathcal{E}, \quad \text{(A9)}$$

the two coupled equations may be brought into a single second-order equation, which can take two distinct forms depending on which two variables are chosen to be independent. Using φ and T as independent variables, one has

$$\frac{\partial^2(\mathcal{E}f_0)}{\partial\varphi^2}-\frac{1}{\mathcal{E}_0}\frac{\partial(\mathcal{E}f_0)}{\partial T}-\frac{\partial}{\partial\varphi}\left(\frac{\mathcal{E}f_0}{\varphi-T}\right)-\frac{\mathcal{E}f_0}{F^2\lambda^2}=0. \quad \text{(A10a)}$$

In terms of $\mathcal{E}$ and T, this same equation is

$$\frac{\partial^2 f_0}{\partial\mathcal{E}^2}+\frac{\partial f_0}{\partial\mathcal{E}}\left(\frac{1}{\mathcal{E}}+\frac{1}{\mathcal{E}_0}\right)+f_0\left(\frac{1}{\mathcal{E}\mathcal{E}_0}-\frac{1}{r\mathcal{E}_r\mathcal{E}_0}\right)-\frac{\partial f_0}{\partial T}=0. \quad \text{(A10b)}$$

Diffusion Solution

Two special cases, field-independent diffusion and steady-state drift, can be obtained at once from Eq. (A10). Multiplying Eq. (A10a) by F^2 and taking $F=0$ we find

$$\frac{\partial^2 Q}{\partial x^2}-\frac{r\mathcal{E}_r}{\lambda^2}\frac{\partial Q}{\partial T}-\frac{Q}{\lambda^2}=0, \quad \text{(A11)}$$

where $Q=\mathcal{E}f_0$ is the slowing down density of Fermi's "age theory."[9] Equation (A11) is simply a "diffusion" equation with an absorption term. The "diffusion constant" is $\lambda^2/r\mathcal{E}_r$ since time is expressed in terms of the number of collisions $T/\mathcal{E}_r$. Except for the last term which results in absorption, the solution is expressed as a function of the "age" τ, the product of the diffusion constant and time, as

$$Q=Q(x^2/\tau), \quad \text{(A12)}$$

where

$$\tau=\lambda^2T/r\mathcal{E}_r. \quad \text{(A13)}$$

Equation (A11) was solved by Hebb[10] without the absorption term for the case of an electron entering a slab of material at $x=0$ with an energy $\mathcal{E}=\varphi$. The boundary conditions are $Q=0$ at $x=-\infty$ and all electrons that reach the position $x=L$ are removed from the layer (emitted). The solution is then

$$Q=(4\pi\tau)^{-1/2}\{\exp(-x^2/4\tau)$$
$$-\exp[-(x-2L)^2/4\tau]\}\exp(-\tau/\lambda^2), \quad \text{(A14)}$$

where the absorption term has been added to Hebb's result.

---

[9] E. Fermi, *Nuclear Physics* (Chicago University Press, Chicago, Illinois, 1950).

[10] M. H. Hebb, Phys. Rev. **81**, 702 (1951).

Drift Solution

The steady-state drift solution can be obtained from Eq. (A10b) by removing the x dependence. The derivative with respect to T vanishes for $x\to\infty$ and finite $\mathcal{E}$ since T can then be replaced by $\varphi=Fx$. The remaining equation was solved by Wolff under the assumption that $\mathcal{E}\gg\mathcal{E}_0$ and $\mathcal{E}\gg r\mathcal{E}_r$, so as to describe electrons with energies above $\mathcal{E}_i$. For his choice of parameters ($r\ll1$) the assumption is valid. A more complete solution of the equation in terms of confluent hypergeometric functions shows that even when these conditions are not completely satisfied ($r>1$) the exponential dependence of f_0 is still that given by Wolff, i.e.,

$$f_0=\text{const}\exp\{-[\tfrac{1}{2}+(\tfrac{1}{4}+\mathcal{E}_0/r\mathcal{E}_r)^{1/2}]\mathcal{E}/\mathcal{E}_0\},\quad\text{(A15)}$$

but the multiplying factor has a somewhat different energy dependence leading to an error, in using Eq. (A15), of 25% in the worst case. We observe that in the absence of ionization, i.e., $r\to\infty$, the solution has the simple temperature $\mathcal{E}_0$, where $\mathcal{E}_0$, however, becomes $\mathcal{E}_1=F^2l_r^2/3\mathcal{E}_r$.

Complete Solution

The solution to the whole of Eq. (A10) can only be obtained in closed form as an approximation. Considering now a given value of field, there are two distinctly different groups of electrons whose initial transient behavior is described by Eq. (A10). The first group consists of those which at large x have small values of $\mathcal{E}$, and, thus, form the steady-state drift electrons. Electrons in the other group have low energy loss to collisions (i.e., small T) and are those of interest to the problem outlined in Sec. I. This distinction between groups, with emphasis on drift and diffusion, respectively, must be made because the exact solution to Eq. (A10) cannot be obtained and the particular approximations made will restrict the solution to the low-energy-loss group. Although the variables φ and T form the natural variables for the solution for low-energy-loss electrons, the somewhat simpler form of Eq. (A10b) makes the approximate solution in terms of the variables $\mathcal{E}$ and T more attractive. We shall take the Laplace transform of this equation with respect to T, in which case the initial value of f_0 in the $\partial f_0/\partial T$ term vanishes for a delta function in f_0 at $\mathcal{E}=T=0$ or by Eq. (A9) at $x=0$. This delta function corresponds to the release of electrons with zero energy at the start of the junction. The remaining equation is similar to that solved for the steady-state drift by means of the confluent hypergeometric function but now the inverse transform is required. Intermediate to the approximation used by Wolff and the complete solution is an approximate form in terms of the modified Bessel function, which affords a somewhat better approximation than that of Wolff. We, therefore, define

$$\Psi(\mathcal{E},s)=\frac{\exp(\mathcal{E}/2\mathcal{E}_0)}{\mathcal{E}_0^2}\int_0^\infty e^{-sT}f_0(\mathcal{E},T)dT,\quad\text{(A16)}$$

from which we obtain for our boundary condition

$$\partial f_0/\partial T=\exp(-\mathcal{E}/2\mathcal{E}_0)s\Psi.\quad\text{(A17)}$$

The effect of the factor $\exp(\mathcal{E}/2\mathcal{E}_0)$ is to reduce Eq. (A10b) to

$$\frac{d^2\Psi}{d\mathcal{E}^2}+\frac{1}{\mathcal{E}}\frac{d\Psi}{d\mathcal{E}}-\left(s+\frac{1}{4}+\frac{\mathcal{E}_0}{r\mathcal{E}_r}-\frac{\mathcal{E}_0}{2\mathcal{E}}\right)\frac{1}{\mathcal{E}_0^2}\Psi=0.\quad\text{(A18)}$$

Requiring f_0 (or Ψ) to go to zero at infinite energy we obtain under the condition $2\mathcal{E}\gg r\mathcal{E}_r$ the approximate solution

$$\Psi\cong\text{const}K_0\left[\frac{\mathcal{E}}{\mathcal{E}_0}\left(s+\frac{1}{4}+\frac{\mathcal{E}_0}{r\mathcal{E}_r}\right)^{1/2}\right],\quad\text{(A19)}$$

and the inverse transform

$$f_0(\mathcal{E},T)\cong\text{const}\frac{\exp(-\mathcal{E}/2\mathcal{E}_0)}{T}\times\exp\left[-\frac{\mathcal{E}^2}{4\mathcal{E}_0T}-\frac{T}{\mathcal{E}_0}\left(\frac{1}{4}+\frac{\mathcal{E}_0}{r\mathcal{E}_r}\right)\right].\quad\text{(A20)}$$

Using the more natural variables φ and T, we may write

$$f_0(\varphi,T)=\frac{\text{const}}{T}\exp\left(-\frac{\varphi^2}{4\mathcal{E}_0T}-\frac{T}{r\mathcal{E}_r}\right).\quad\text{(A21)}$$

We see from the approximation involved in obtaining Eq. (A19), i.e., $2\mathcal{E}\gg r\mathcal{E}_r$, that we have, indeed, the group of electrons with high energies. The solution, in fact, does not go over into the steady-state drift solution at x (or T) $\to\infty$, because we have not resupplied the distribution with those electrons which were absorbed by ionization.